Intervening Attenuation Affects First-order Statistical Properties of Ultrasound Echo Signals

James A. Zagzebski, Jian-Feng Chen, Fang Dong, and Thaddeus Wilson

Abstract—**Previous studies show that first-order statistical properties of ultrasound echo signals are related to the effective number of scatterers in the "resolution cell" of a pulse-echo ultrasound system. When the effective number of scatterers is large ($\sim$ 10 or more) this results in echo signals whose amplitude follows a Rayleigh distribution, with the RF echo signal obeying Gaussian statistics; deviation from Rayleigh or Gaussian statistics yields information on scatterer number densities. In this paper, the influence of the medium's attenuation on non-Gaussian properties of the echo signal is considered. Preferential attenuation of higher frequency components of a pulsed ultrasound beam effectively broadens the beam and increases the resolution cell size. Thus, the resultant non-Gaussian parameter for broad bandwidth excitation of the transducer depends not only on the scatterer number density but also on the attenuation in the medium. These effects can be reduced or eliminated by using narrow-band experiments.**

I. Introduction

In an earlier paper [1] parameters expressing the non-Gaussian and the non-Rayleigh properties of ultrasound echo signals were derived. The parameters are obtained from ratios of the fourth moment to the square of the second moment of either the instantaneous echo signal or the echo signal amplitude. Their values are related to the degree to which M_{eff}, the number of scatterers contributing to the instantaneous echo signal, falls below the number needed for Rayleigh or Gaussian statistics to apply. M_{eff} is determined by the beam width and pulse duration of the transducer and the scatterer number density in the medium. Rayleigh or Gaussian statistics apply when M_{eff} is approximately 10 or higher [2], [3].

Various groups have explored non-Gaussian or non-Rayleigh statistics for ultrasound tissue characterization. Sleefe and Lele [4] used the fourth and second moments of the echo signal voltage to estimate scatterer number densities in tissue. Shankar *et al.* [5] applied parameters derived from non-Rayleigh echo signal statistics to distinguish normal breast tissue from breast tumors. That work was extended to compute both the number of scatterers and the distribution of scattering cross-sections in insonified volumes [6]. We have applied and tested similar methods to compute a frequency-dependent effective scatterer number density in tissue-like samples [7], [8].

Although the scatterer number density and information regarding scatterer size distributions are embedded in the non-Rayleigh and non-Gaussian parameters [8], it is important to keep in mind that system and transmission path dependencies also influence these determinations. Specifically, the effects of intervening attenuation between the transducer and region of interest often are ignored. Experiments described in this paper were intended to evaluate whether this omission is justified. Because the resolution cell-size for a pulsed ultrasound beam varies with the amount of attenuation in the medium [10], differences in intervening tissue attenuation could have a significant effect on any statistical parameter estimated from a region in the beam.

We will review briefly the basis for the non-Rayleigh and the non-Gaussian parameters. Then results of experiments will be presented to examine attenuation dependencies on these parameters.

II. Overview of the Non-Gaussian and Non-Rayleigh Parameters

When a pulsed transducer insonifies a medium containing sparse, randomly distributed scatterers, the complex echo signal $U(t)$ can be represented as a superposition of signals due to all scatterers in the beam. That is [1],

$$U(t) = \sum_{j=1}^{M_t} u_j(\vec{r}_j, t) \tag{1}$$

where the sum is over all scatterers that contribute to the echo signal at time t, and $u_j(\vec{r}_j, t)$ represents the complex echo signal from the jth scatterer. Using the notation presented in [1], this can be represented by:

$$u_j(\vec{r}_j, t) = \int_0^\infty d\omega T_o(\omega) A_o(\omega) \psi_j(\omega) e^{-i\omega t} A^2(\vec{r}_j, \omega) \tag{2}$$

where $T_o(\omega)$ is a complex transfer function relating the net instantaneous force on the transducer at the angular frequency ω to the detected voltage, $A_o(\omega)$ is a complex

Manuscript received January 30, 1997; accepted August 5, 1998. This work was supported in part by NIH RO1-CA39224 and by the Wisconsin Clinical Cancer Center.

J. A. Zagzebski, F. Dong, and T. Wilson are with the Department of Medical Physics, University of Wisconsin, Madison, WI 53706 (e-mail: jimzag@macc.wisc.edu).

J.-F. Chen is with Siemens Medical Systems, Issaquah, WA 98027-7002.

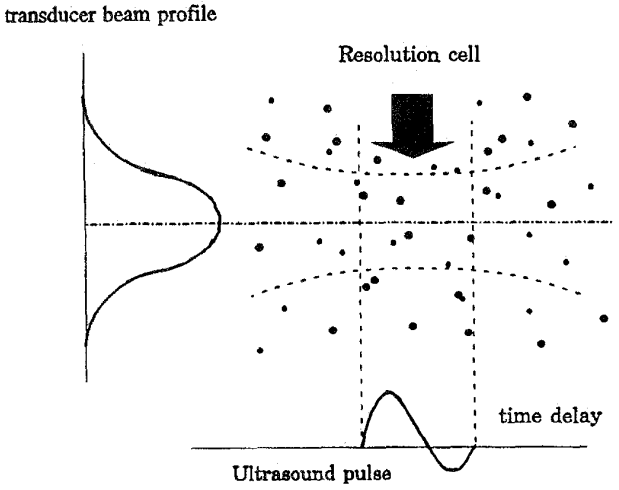

Fig. 1. Schematic of the resolution cell for a pulse-echo ultrasound experiment. The volume is established by the beam cross-sectional area and the transducer pulse duration.

superposition coefficient corresponding to the frequency composition of the emitted pulse, $\psi_j(\omega)$ is the value of the angular distribution factor at a 180° scattering angle for the jth scatterer at position $\vec{r}_j$ [11] and $i \equiv \sqrt{-1}$.

The scatterers, M_t which significantly contribute to the echo signal in (1) are located in a volume, $\Delta\Omega_t$, defined by the ultrasound field produced by the transducer, $A(\vec{r}_j, \omega)$, and the ultrasound pulse, as shown schematically in Fig. 1. $A(\vec{r}_j, \omega)$ is given by [1]:

$$A(\vec{r}_j, \omega) \equiv \iint_S ds' \frac{e^{i\frac{\omega}{c}|\vec{r}_j - \vec{r}'|}}{|\vec{r}_j - \vec{r}'|} e^{-\alpha_1(\omega)|\vec{r}_j - \vec{r}'|}$$

where $\vec{r}'$ points to area element ds' on the transducer surface S, c is the speed of sound and $\alpha_1(\omega)$ is the frequency-dependent attenuation coefficient in the medium.

When their positions are independent, the number of scatterers within $\Delta\Omega_t$ follows the Poisson distribution. Then, the kurtosis of the echo signal envelope, that is, the ratio of the fourth moment to the square of the second moment of the envelope, is given by

$$\frac{\langle |U(t)|^4 \rangle}{\langle |U(t)|^2 \rangle^2} \simeq 2\left(1 + \frac{1}{\alpha}\right) \tag{3}$$

where $\langle \ldots \rangle$ designates the ensemble average of the echo signals for different transducer positions. α is called the non-Rayleigh parameter, given by [1]:

$$\frac{1}{\alpha} = \frac{1}{2\langle N \rangle} \times \frac{\iiint_{\Delta\Omega_t} d\vec{r} \langle |u(\vec{r}, t)|^4 \rangle_s}{\left\{ \iiint_{\Delta\Omega_t} d\vec{r} \langle |u(\vec{r}, t)|^2 \rangle_s \right\}^2} \tag{4}$$

Here $\langle N \rangle$ is the scatterer number density in the medium and $\langle |u(\vec{r}, t)|^n \rangle_s$ designates an ensemble average over all scatterers of the nth moment of $u(\vec{r}_j, t)$. A complete derivation may be found in [1].

Similarly, the kurtosis computed for the time domain, radio frequency (RF) signal is given by [1]:

$$\frac{\langle |V(t)|^4 \rangle}{\langle |V(t)|^2 \rangle^2} \simeq 3\left(1 + \frac{1}{\beta}\right) \tag{5}$$

where

$$\frac{1}{\beta} = \frac{1}{3\langle N \rangle} \times \frac{\iiint_{\Delta\Omega_t} d\vec{r} \langle |v(\vec{r}, t)|^4 \rangle_s}{\left\{ \iiint_{\Delta\Omega_t} d\vec{r} \langle |v(\vec{r}, t)|^2 \rangle_s \right\}^2} \tag{6}$$

and $v(\vec{r}, t) \equiv \mathrm{Re}\, u(\vec{r}, t)$.

When the scatterer number density and/or the resolution cell volume is large, $1/\beta \to 0$. The statistical properties of the RF echo signal approach those of the Gaussian distribution, and the ratio of the fourth moment to the square of the second moment of the echo signal goes to 3.0. Similarly, the ratio of the fourth moment to the square of the second moment of the echo signal envelope (3) goes to 2.

Let us restrict the remaining discussion to the statistical properties of the RF echo signal. The non-Gaussian parameter, $1/\beta$, will be greater than zero for sparse scattering conditions. When this is the case, data reduction schemes may be used to estimate the scatterer number density and related parameters [4]–[9].

The effect of intervening attenuation between the transducer and the region from which echo data are recorded is embodied in terms in the volume integrals on the right-hand side of (6), which include the transducer field, $A(\vec{r}_j, \omega)$. For broad bandwidth, clinical-type ultrasound pulses, attenuation preferentially removes higher frequency components in the beam. The remaining, lower frequencies will result in a broader beam compared to an unattenuated beam [10]. Thus, a high level of attenuation between the transducer and the sample volume is expected to increase the number of scatterers contributing to the echo signal, decreasing $1/\beta$ in (6).

III. Experimental Methods

Attenuation effects on $1/\beta$ were investigated using two experimental approaches. Experiment 1 measured this parameter when samples with the same scatterer number density but different levels of attenuation were placed in water near the focal region of a transducer [see Fig. 2(a)]. Most of the path between the transducer and region of interest in the sample was water, but the final 2 cm consisted of an attenuating path, the degree of attenuation varying between samples.

A second experiment applied differing amounts of attenuation to the entire path between the ultrasound transducer and the region of interest. Signals were recorded from

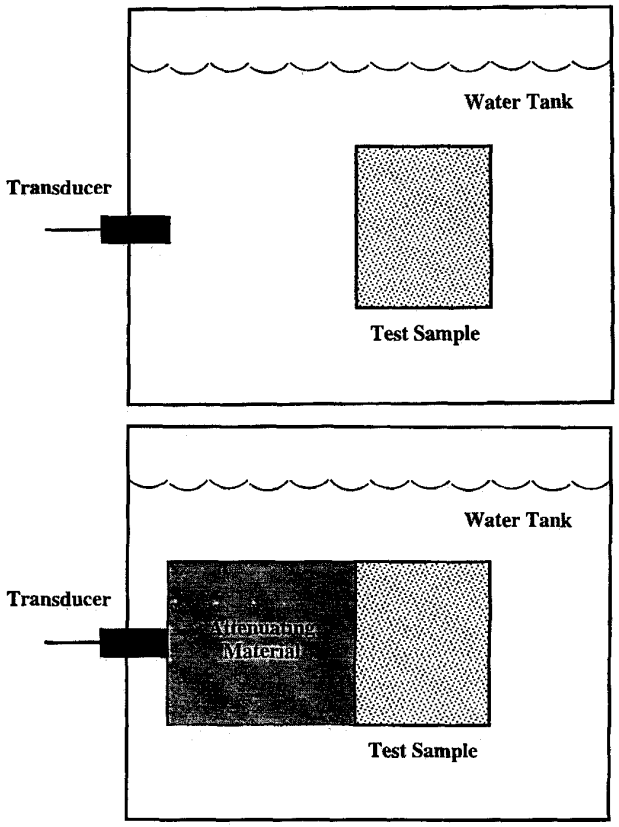

Fig. 2. (top): Experimental arrangement for recording echo signals from samples in experiment 1. The test samples were placed in the focal region of the transducer in water. (bottom): Experimental arrangement for recording echo signals from a sample in experiment 2. The transducer was placed either in contact with the surface of the phantom, or in contact with 6-cm long off-set pads having lower attenuation coefficient than the phantom block itself.

near the focal region of a transducer [Fig. 2(b)], but different attenuation blocks were placed between the transducer and sample. This approach more closely mimics situations that might be encountered if these methods were applied clinically than the set up in Fig. 2(a).

Three test samples were used for experiment 1. Samples consist of tissue-mimicking gel with randomly positioned 80 μm glass beads to provide scattering. Each sample has the same glass bead concentration, 400 cm^{-3}. The samples differed in attenuation, which was controlled by adding specific amounts of graphite powder before the gel congealed [12]. No powder yielded a very low attenuation coefficient ($\approx$ 0.04 dB/cmMHz); 30 grams graphite per liter of molten gel yielded a nominal value of 0.3 dB/cmMHz, and 60 grams of graphite per liter yielded approximately 0.6 dB/cmMHz.

Test samples were placed in the focal region of a single element, 5.0 MHz focused transducer. It has an 18.6 mm diameter aperture and a radius of curvature of 8.5 cm. The transducer was excited with either a single-cycle 5 MHz waveform for broad-band excitation or an eight-cycle 5 MHz burst, yielding a narrow bandwidth pulse. Resultant echo signal waveforms were digitized in a LeCroy 9400 digital oscilloscope with a 100 MHz sampling frequency. Five-microsecond data segments were acquired from 80 statistically independent transducer positions, with 4 mm lateral translations of the phantoms between recordings. Echo data were stored on a PC computer disk for off-line analysis.

Experiment 2 involved recording echo signals from near the focal region of the transducer, but with different amounts of attenuation in the entire path between the transducer and the region of interest. A large tissue mimicking phantom (12 cm $\times$ 12 cm $\times$ 16 cm), containing the same concentration of glass bead scatterers as the previous three test samples (400 cm^{-3}) was used. Its attenuation coefficient is 2.75 dB/cm at 5 MHz. Echo signals were recorded with the 5 MHz transducer described earlier, using only broad-band excitation. Again, 5-μs signal segments were digitized, this time with the region of interest centered at depths of 8 cm, 8.5 cm, 9 cm, and 9.5 cm from the transducer surface. Initially, the transducer was placed in direct contact with the phantom surface; this provided the most severe attenuation between the transducer and region of interest. Then, echo data were recorded when 6-cm offset blocks were placed between the transducer and the phantom surface [Fig. 2(b)]. Block 1 is of clear agar, which has an attenuation coefficient of 0.23 dB/cm at 5 MHz. Block 2 has an attenuation coefficient of 1.32 dB/cm at 5 MHz.

For each experiment, the kth moment $\langle |V(t)|^k \rangle$, of the RF echo signal was computed from the region of interest using:

$$\langle |V(t)|^k \rangle = \frac{\sum_{\ell=1}^{W} \sum_{m=1}^{P} v_{\ell,m}^k}{W \times P}$$

where $v_{\ell,m}$ is the value of the digitized echo signal for transducer position ℓ and sample point m, W is the number of transducer positions from which echoes were recorded and P is the number of digitized sample points for each transducer location. Then the quantity $1/\beta$ was computed using (5).

IV. Results

Fig. 3 shows the echo signal power spectra obtained from the test samples in experiment 1. Samples with higher attenuation values undergo not only an overall attenuation of the spectra, but also a preferential attenuation of higher frequency components because of the approximately linear relationship between the attenuation coefficient and ultrasonic frequency in these materials.

Values of $1/\beta$ for these samples are listed in Table I. Here the $\pm$ values indicate standard deviations of results among data for all 80 transducer positions. The sample with the least attenuation (0.45 dB/cm) has the highest $1/\beta$, reflecting the greatest departure from Gaussian statistics among the three test samples; evidently, the ultra-

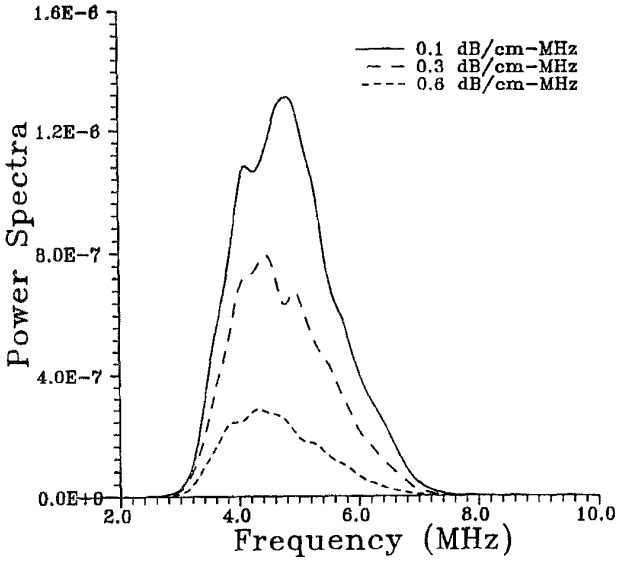

Fig. 3. Echo signal power spectra recorded from test samples in experiment 1. Samples having higher attenuation resulted in lower amplitude signals and a shifting of the center frequency of the power spectrum to lower frequencies.

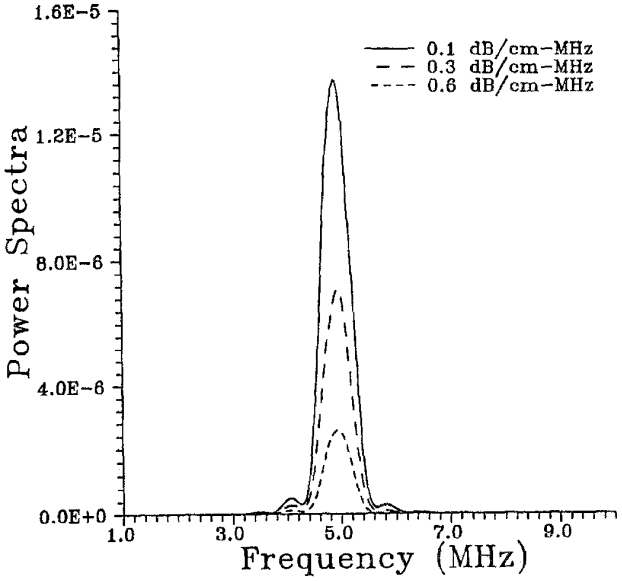

Fig. 4. Same as Fig. 3, only for narrow bandwidth excitation of the transducer.

TABLE I

$1/\beta$ VALUES FOR SAMPLES IN EXPERIMENT 1. SAMPLE ARE LABELED BY THEIR ATTENUATION COEFFICIENT AT 5 MHz. RESULTS ARE SHOWN BOTH FOR BROAD BANDWIDTH AND NARROW BANDWIDTH EXCITATION OF THE TRANSDUCER.

	$1/\beta$		
Sample:	0.45 dB/cm	1.8 dB/cm	3.24 dB/cm
Broad bandwidth	1.9 ± 0.1	1.4 ± 0.1	1.0 ± 0.1
Narrow bandwidth	0.57 ± 0.1	0.63 ± 0.1	0.53 ± 0.1

sound beam is narrowest, consequently the fewest number of scatterers contribute to the echo signal for this sample. The remaining two samples have the same scatterer number density, but they have progressively higher attenuation coefficients. Their $1/\beta$ values are lower than the less attenuating sample.

The longer attenuating path in the large phantom has a similar effect on $1/\beta$ values. Table II presents results from experiment 2; again standard deviations are shown with values for $1/\beta$. At the transducer focal distance (8.5 cm), we recorded a value of $1/\beta$ of 1.55 for the path with the lowest amount of attenuation. Notice, $1/\beta$ changes with depth, evidently reflecting changes due both to the focusing effect of the transducer and to the effects of different amounts of attenuation. By exchanging the first 6 cm of the beam path with material having a progressively higher attenuation coefficient, the value of $1/\beta$ at 8.5 cm gradually decreases. This evidently reflects the fact that there is more spreading of the ultrasound beam when higher amounts of tissue-like attenuation are present in the beam path.

If the major source of these changes is frequency filtering caused by attenuation, one way to offset the effects would be to use narrower bandwidth measurements. Fig. 4 presents analogous spectra as in Fig. 3 for experiment 1 samples, only these spectra resulted from the narrow bandwidth excitation of the transducer. The shapes of the power spectra are nearly identical for the different samples when narrow-band pulses are used.

The lower portion of Table I lists $1/\beta$ values from the three test samples for the narrow bandwidth excitation. For each sample, $1/\beta$ is lower than the value for broad bandwidth excitation, evidently because of the greater volume of tissue contributing to the instantaneous signal value with the longer duration pulses. For narrow bandwidth excitation, $1/\beta$ does not change with the amount of attenuation in the sample.

V. DISCUSSION

The non-Gaussian parameter $1/\beta$ as described in this paper, and parameters related to it such as the scatterer number density and even the clustering parameter suggested by Weng *et al.* [9], may have value in ultrasound diagnosis. Various researchers have seen differences in these computed parameters for different types of tissue and for normal tissue vs malignant tumors.

The parameter $1/\beta$ is closely related to the effective number of scatterers contributing to the echo signal over the frequency band of the interrogating ultrasound pulse. When the effective number is large (say, greater than 10), $1/\beta$ approaches zero and the RF echo signal follows Gaussian statistics, with a kurtosis of 3. The effective number of scatterers depends on the volume occupied by the ultrasound pulse giving rise to the instantaneous value of

TABLE II

$1/\beta$ VALUES FROM A 400 SCATTERER CM^{-3} PHANTOM HAVING A 6-CM ATTENUATING BLOCK BETWEEN THE TRANSDUCER AND PHANTOM SURFACE. DATA WERE RECORDED AT AXIAL DISTANCES OF 8 CM, 8.5 CM, 9 CM, AND 9.5 CM FROM A 5 MHz, 18.6 MM DIAMETER, 8.5 CM RADIUS OF CURVATURE TRANSDUCER FOLLOWING BROAD BANDWIDTH EXCITATION. RESULTS ARE SHOWN FOR THREE DIFFERENT ATTENUATION COEFFICIENTS OF THE MATERIAL IN THE ATTENUATING BLOCK.

	$1/\beta$			
Attenuation of first 6-cm of path (dB/cm at 5 MHz)	8 cm	8.5 cm	9 cm	9.5 cm
0.25	1.52 ± 0.13	1.55 ± 0.2	1.39 ± 0.2	1.34 ± 0.2
1.65	1.35 ± 0.1	1.26 ± 0.1	1.36 ± 0.2	1.27 ± 0.2
2.25	1.19 ± 0.1	1.16 ± 0.1	1.24 ± 0.1	1.22 ± 0.1

the echo signal. For the short duration, broad-band excitation in experiments described in this paper, the -6 dB beam width in the focal region of the transducer is approximately 2 mm. This yields a beam cross-sectional area and a pulse volume of ~ 3.1 and ~ 2 mm^3, respectively. For the 400 scatterers per cm^3 phantom, this means that approximately 1 to 2 scatterers contributed to the instantaneous value of the echo signal for the narrowest portion of the unattenuated beams. Thus, it should be expected that $1/\beta > 0$ for these experimental conditions, and data in Tables I and II show this is the case.

The 8-cycle excitation pulse applied during the narrow bandwidth measurements in experiment 1 resulted in a larger axial extent for the pulse volume than the broad bandwidth measurements. This is accompanied by lower $1/\beta$ values for each sample, as expected. Likewise, the axial location of the region of interest when focused transducers are used, as well as the settings of the focusing pattern of array transducers, would influence $1/\beta$.

The present study demonstrates that differences in intervening attenuation between the transducer and region of interest will have an effect on $1/\beta$. Higher attenuation values widen the beam of broad bandwidth pulsed transducers [10], resulting in a greater pulse volume and more scatterers contributing to the instantaneous ultrasound signal. This is reflected in the broad bandwidth measurements reported in Tables I and II; $1/\beta$ decreases for samples having increased attenuation, even though the scatterer number density is the same in the samples.

It might be possible to correct for these effects, if the attenuation in the intervening material can be measured. Possible methods for accounting for attenuation effects might be to estimate or measure the ultrasound attenuation using methods described in the literature [13], [14] and then apply modeling; the latter could be done by inserting the measured attenuation coefficient into the expression for $A(\vec{r}_j, \omega)$ in (2) and propagating the effect of an increased attenuation using (6). Alternatively, an effective scatterer number density might be obtained using a reference phantom method, where the reference has a known scatterer number density. References having different degrees of attenuation but the same scatterer number density could be used, and kurtosis values of the sample compared with kurtosis values from the same depth in the reference that has approximately the same attenuation as the sample. Equivalent attenuation between sample and reference could be judged by comparing variations of echo signal amplitude with depth.

Another approach to overcome effects of attenuation would be to use narrow band measurements. Fig. 4 demonstrates that the spectral shape is unchanged in the presence of attenuation if narrow band excitation is used, and Table I, (line 3) shows that the effect of attenuation on corresponding $1/\beta$ values is negligible. Although $1/\beta$ is smaller than it is for broad bandwidth excitation, reflecting a larger effective sample volume, the results are approximately the same for the different attenuating samples. Narrow band measurements can be done using long duration pulses, as in the present paper, or by filtering the echo signals following broad band excitation, as in [13]. A disadvantage of this approach is that the pulse volume would increase, increasing M_{eff}. This in turn increases the statistical uncertainty of the scatterer number density estimator [15], [16].

VI. CONCLUSION

The influence of acoustic attenuation on the statistical properties of ultrasonic echo signals was studied using tissue-mimicking phantoms. Samples having the same scatterer number density but different amounts of attenuation were interrogated with pulses from a 5 MHz focused transducer. The non-Gaussian parameter, $1/\beta$ recorded in the focal region decreased when the attenuation in the path between the transducer and region of interest increased. This finding is consistent with previous reports that beam widths of broad bandwidth transducers increase near the focal region when higher amounts of tissue-like attenuation are placed in the beam path. These attenuation effects were substantially reduced when narrow bandwidth pulses were applied during data acquisition. Possible effects of intervening attenuation must be considered when applying these statistical methods.

ACKNOWLEDGMENTS

We are grateful to Dr. Ernest Madsen and Mr. Gary Frank for assistance in constructing the phantoms.

REFERENCES

[1] J.-F. Chen, J. A. Zagzebski, and E. L. Madsen, "Non-Gaussian versus non-Rayleigh statistical properties of ultrasound echo signals," *IEEE Trans. Ultrason., Ferroelect., Freq. Contr.*, vol. 41, pp. 435–440, 1994.

[2] T. A. Tuthill, R. H. Sperry, and K. J. Parker, "Deviations from Rayleigh Statistics in ultrasonic speckle," *Ultrason. Imaging*, vol. 10, pp. 81–89, 1988.

[3] B. J . Oosterveld, J. M. Thijssen, and W. A. Verhoef, "Texture of B-mode echograms: 3-D simulations and experiments of the effects of diffraction and scatterer density," *Ultrason. Imaging*, vol. 7, pp. 142–160, 1985.

[4] G. E. Sleefe and P. P. Lele, "On estimating the number density of random scatterers from backscattered acoustic signals," *Ultrasound Med. Biol.*, vol. 14, pp. 709–727, 1988.

[5] P. M. Shankar, J. M. Reid, H. Ortega, C. W. Piccoli, and B. B. Goldberg, "Use of non-Rayleigh statistics for the identification of tumors in the ultrasonic B-scan of the breast," *IEEE Trans. Med. Imag.*, vol. 12, pp. 687–692, 1993.

[6] P. M. Shankar, "A model for ultrasonic scattering from tissues based on the K distribution," *Phys. Med. Biol.*, vol. 40, pp. 1633–1649, 1995.

[7] J.-F. Chen, E. L. Madsen, and J. A. Zagzebski, "A method for determination of a frequency-dependent effective scatterer number density," *J. Acoust. Soc. Amer.*, vol. 95, pp. 77–85, 1994.

[8] J.-F. Chen, J. A. Zagzebski, and E. L. Madsen, "Experimental demonstration of the frequency dependence of the effective scatterer number density." *J. Acoust. Soc. Amer.*, vol. 99, pp. 1932–1936, 1996.

[9] L. Weng, J. M. Reid, P. M. Shankar, and K. Soetanto, "Ultrasound speckle analysis based on the K distribution," *J. Acoust. Soc. Amer.*, vol. 89, pp. 2992–2995, 1991.

[10] J. A. Zagzebski, R. A. Banjavic, and E. L. Madsen, "Focused transducer beams in tissue-mimicking material," *J. Clin. Ultrasound*, vol. 10, pp. 159–166, 1982.

[11] P. M. Morse and K. U. Ingard, *Theoretical Acoustics*. Princeton, NJ: Princeton Univ. Press, 1968, Chapter 7, pp. 425–427.

[12] E. L. Madsen, J. A. Zagzebski, R. A. Banjavic, and R. Jutila, "Tissue-mimicking materials for ultrasound phantoms," *Med. Phys.*, vol. 5, pp. 391–394, 1978.

[13] L.-X. Yao, J. A. Zagzebski, and E. L. Madsen, "Backscatter coefficient measurements using a reference phantom to extract depth-dependent instrumentation factors," *Ultrason. Imaging*, vol. 12, pp. 58–70, 1990.

[14] B. S. Garra, M. F. Insana, and T. H. Shawker, "Quantitative estimation of liver attenuation and echogenicity: normal state versus diffuse liver disease," *Radiology*, vol. 162, pp. 61–67, 1987.

[15] J.-F. Chen, J. A. Zagzebski, and E. L. Madsen, "Statistical uncertainty in estimates of an effective scatterer number density for ultrasound," *J. Acoust. Soc. Amer.*, vol. 96, pp. 2556, 1994.

[16] R. F. Wagner, D. G. Brown, K. A. Wear, M. F. Insana, and T. J. Hall, "Statistical properties of the scatterer number density estimator," *Ultrason. Imaging*, vol. 13, p. 192, 1991.

James A. Zagzebski was born in Stevens Point, WI, in 1944. He received the B.S. degree in physics from St. Mary's College, Winona, MN, and the M.S. degree in physics and the Ph.D. degree in radiological sciences from the University of Wisconsin, Madison. He is a professor of medical physics and of radiology and human oncology at the University of Wisconsin.

His research interests include ultrasound imaging and tissue characterization, flow detection, and visualization using ultrasound and technological assessment of imaging devices.

Dr. Zagzebski's professional affiliations include the IEEE, the American College of Radiology, the American Institute of Ultrasound in Medicine, and the American Association of Physicists in Medicine.

Jian-Feng Chen was born in Hangzhou, China. He received the B.S. degree in physics from Tongji University, Shanghai, China, in 1985 and the M.S. and Ph.D. degrees in medical physics from the University of Wisconsin, Madison, in 1992 and 1994, respectively.

Dr. Chen is a senior scientist at Siemens Medical Systems, Inc. His research interests are in general medical physics and medical ultrasound.

Fang Dong was born in NingBo, P.R. China, in 1968. He received a B.S. degree in physics from Fudan University, Shanghai in 1989 and M.S. degrees in solid state physics and medical physics from Ohio University and the University of Wisconsin in 1994 and 1996, respectively. He is currently working toward a Ph.D. degree in medical physics.

His research interests are in ultrasound imaging and digital signal processing.

Thaddeus A. Wilson was born in California in 1969. He received the B.S. degree in electrical engineering from Christian Brothers College, Memphis, TN, in 1991 and the M.S. degree in medical physics from the University of Wisconsin, Madison. He is currently working toward a Ph.D. degree in medical physics.

His research interests are in the field of medical ultrasound imaging and tissue characterization.